DOI 10.1007/s10946-023-10120-2
Journal of Russian Laser Research, Volume 44, Number 2, March, 2023

Q-SWITCHED THULIUM-DOPED FIBER LASER WITH MOLYBDENUM–ALUMINUM-BORIDE-BASED SATURABLE ABSORBER

Abdulkadir Mukhtar Diblawe,[1,2] Bilal A. Ahmad,[3] Kaharudin Dimyati,[1,4] Ahmad Haziq Aiman Rosol,[5] Zian Cheak Tiu,[6] Retna Apsari,[7] and Sulaiman Wadi Harun[1*]

[1] *Department of Electrical Engineering, Faculty of Engineering, University of Malaya Kuala Lumpur 50603, Malaysia*

[2] *Department of Telecommunication Engineering, Faculty of Engineering, Hormuud University Mogadishu 046, Somalia*

[3] *Department of Communication Engineering, Al-Ma'moon University College Al-Washash, 700921 Baghdad, Iraq*

[4] *Department of Engineering, Faculty of Advanced Technology and Multidiscipline Airlangga University Surabaya 60115, Indonesia*

[5] *Malaysia–Japan International Institute of Technology (MJIIT), Universiti Teknologi Malaysia Jalan Sultan Yahya Petra, 54100 Kuala Lumpur, Malaysia*

[6] *Faculty of Engineering and Quantity Surveying, INTI International University Nilai, Negeri Sembilan 71800, Malaysia*

[7] *Department of Physics, Faculty of Science, Airlangga University Surabaya 60115, Indonesia*

[*]Corresponding author e-mail: swharun@um.edu.my

Abstract

We propose and demonstrate a new *Q*-switched thulium-doped fiber laser (TDFL) by utilizing a passive saturable absorber (SA) based on Molybdenum–Aluminium boride (MoAlB). The MoAlB is a metal–ceramic-based material; it is embedded in polyvinyl-alcohol (PVA) material to operate as the SA. The laser successfully generates stable *Q*-switched pulses operating at 1974.7 nm with a maximum repetition rate of 57.7 kHz and a minimum pulse width of 1.79 μs. A maximum pulse energy of 90.2 nJ is recorded at 436 mW pump power. Our experiment is the first demonstration on the use of MoAlB for the pulse laser generation in the 2 μm wavelength region.

Keywords: *Q*-switching, Thulium-doped fiber laser, saturable absorber, Molybdenum–Aluminum boride.

1. Introduction

Q-switched lasers operating in a mid-infrared region (MIR) of 2 μm has gained great interest due to their potential in many applications including optical communication, materials processing, spectroscopy, and light detection and ranging (LIDAR) [1–5]. The 2 μm laser operation can be obtained, using a

Manuscript submitted by the authors in English on November 16, 2022.

Thulium-doped fiber (TDF) or Thulium–Holmium co-doped fiber (THDF) as an active medium. The Q-switching in this wavelength region can be passively realized, using a saturable absorber (SA) device to modulate the Q-factor of the laser cavity. There are many reported SAs that have successfully induced Q-switching operation, such as semiconductor saturable absorber mirrors (SESAMs), graphene, topological insulators (TIs), transition-metal dichalcogenides (TMDs), and black Phosphorus (BP). These SAs have proven its feasibility to generate Q-switched laser operation across the $1-2$ μm bandwidth region.

In the early stage of SA development, SESAMs were used as promising SA materials for fiber-laser applications [6]. Unfortunately, the nature of high fabrication cost and low damage threshold constrained commercial applications of SESAMs [7]. With the exploration of 2D materials, graphene has been utilized as a SA. The low modulation depth and zero band gap are the major drawbacks of graphene [8], in spite of its fantastic characteristics, such as a wide operation bandwidth and a fast recovery time [9]. Successively, the development of SA using 2D materials has extended to TIs, TMDs, and BP. TIs materials including Sb_2Te_3 [10], Bi_2Te_3 [11], and Bi_2Se_3 [12] were used in achieving laser pulses operating in various wavelength spans [13, 14], but TIs suffer from chemical reactivity and structural instability [15]. TMDs showed unique absorption properties, which were demonstrated through Tungsten disulfide (WS_2) [16], Molybdenum disulfide (MoS_2) [17], $MoTe_2$ [18], and WSe_2 [19]. However, they suffer from complex fabrication processes and low optical damage threshold [20]. BP was utilized in many fiber-laser pulse applications [21], due to its broadband nonlinear optical response and the ease of fabrication. Nevertheless, this material undergoes a quick damage, when it is exposed to Oxygen or water [22].

The development of SA has extended to other nanomaterials that providing outstanding electrical and optical properties. Recently, a metal–ceramic MAX phase materials have gained tremendous interests for numerous applications in various areas, including aerospace and nuclear engineering [23,24]. MAX phases are precursors to produce MXenes, and this material has demonstrated exciting potential in photonics applications. MAX phases exhibit excellent material properties, such as high damage tolerance, excellent electrical conductivity, good thermal-shock resistance, and machinability [25]. Due to the nature of ceramic, MAX phase materials are relatively lighter and great oxidation resistant. In this work, a family member of MAX phase, Molybdenum–Aluminium boride (MoAlB) has been proposed as SA material for operation in the 2 μm region. The MoAlB has been experimentally integrated in a fiber-laser system to induce the Q-switching operation at the 1974.69 nm wavelength. The SA film was fabricated by blending MoAlB solution within a host polymer of polyvinyl alcohol (PVA). By incorporating the MoAlB-PVA film into the TDFL cavity, we obtained stable short pulses with a shortest pulse width of 1.79 μs and a pulse energy of 90.2 nJ. To our knowledge, this is the first time that MoAlB-based SA is utilized to produce passively Q-switched laser pulses in the 2 μm region.

2. Preparation and Characterization of the MoAlB SA

The SA film was fabricated by blending a solution of MoAlB material within a host polymer of PVA. The PVA was chosen due to its great physical characteristics and chemical resistance [26]. The MoAlB powder acquired from Laizhou Kai Kai Ceramic Materials Co., Ltd, China is used in this work. This material has a phase purity of more than 96%, and particle size of less than 200 nm. At first, we obtained the PVA liquid by resolving of PVA powder (1 g) to 100 ml of distilled water. The solution was stirred for 2 h. using magnetic stirrer at 300 rpm speed and a temperature of 100°C, until the PVA powder was completely liquefied. Next, 10 mg of MoAlB powder was add up into 10 ml of the prepared PVA solution. The MoAlB PVA solution was stirred constantly for 168 h. at a speed of 300 rpm, using a

magnetic stirrer to make sure that the composite solution was completely dissolved. Finally, we put the dispersed solution into a petri dish and make it to dry by leave it at room temperature for 48 h. or more, that resulted in the formation of MoAlB thin film with a thickness of about 60 μm. We illustrate the preparation of the MoAlB thin film in Fig. 1.

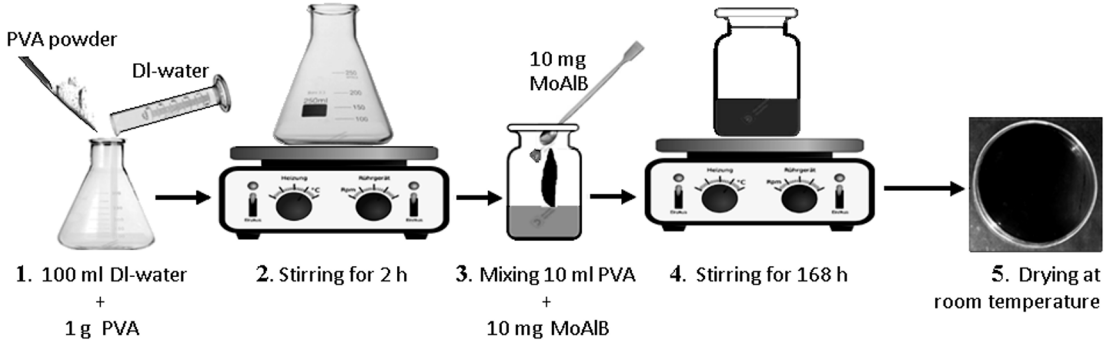

Fig. 1. The preparation of MoAlB thin film.

We investigated the morphological structure of MoAlB thin film, using scanning electron microscopy (SEM) analysis; see Fig. 2 a. The SEM image shows the particles of MoAlB are equally dispersed inside the PVA host. The thin film is examined, using an energy-dispersive X-ray spectroscopy (EDX) analysis to confirm the presence of MoAlB molecules. The result of the analysis is illustrated in Fig. 2 b, where there are clearly presented several peaks corresponding to Molybdenum (Mo), Boron (B), and Aluminum (Al) elements. In Table in Fig. 2 b, one can see that the composition of Mo, B, and Al are 61.43 wt.%, 23.94 wt.%, and 14.62 wt.%, respectively. MoAlB-SA is prepared by cutting the thin film into pieces and sandwiched between the fiber ferrule made of a standard single-mode-fiber (SMF-28 type) FC/PC pigtail with the aid of index matching gel.

a)

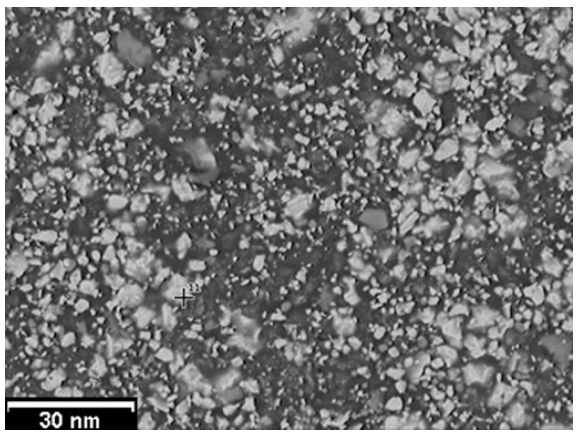

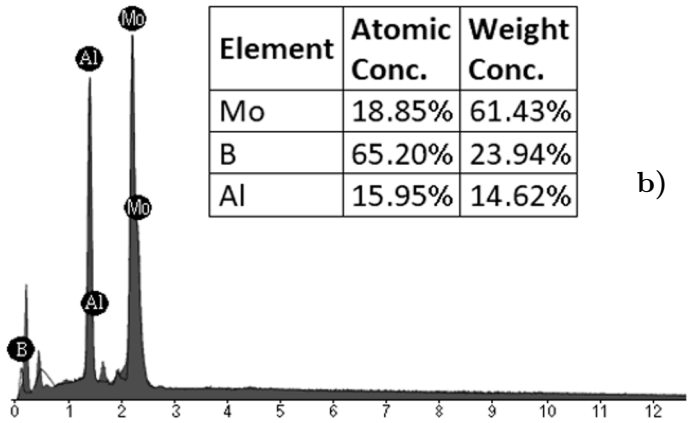

Element	Atomic Conc.	Weight Conc.
Mo	18.85%	61.43%
B	65.20%	23.94%
Al	15.95%	14.62%

b)

Fig. 2. Material characterization results; here, the SEM image (a) and the EDX spectrum (b).

3. Cavity Configuration

The schematic diagram of the TDFL configuration utilizing MoAlB as SA is given in Fig. 3. The MoAlB thin film is slot in between two fiber ferrules, which is then connected by a fiber adaptor. It

forms an SA device, which can be easily incorporated into a TDFL ring cavity. The ring resonator comprises of a 1552 nm pump laser, a wavelength division multiplexer (WDM), a 5 m long Thulium-doped fiber (TDF), and 90/10 output coupler (OC). The pump laser is based on an Erbium–Ytterbium-doped fiber laser (EYDFL) operating at 1552 nm; its output power is regulated by a laser diode controller (Arroyo Instrument: 4308). The TDF employed as an active fiber is a commercial fiber (Nufern, SM-TSF). It has a 9/125 core/cladding geometry, a numerical aperture (NA) of 0.16, a cut-off wavelength of 1750 nm, and a 27 dB/m absorption loss at the 793 nm wavelength. A 90/10 OC is used to allow 90% of the laser beam oscillating inside the ring cavity and extract 10% from the cavity for further analysis. At the output port, a 5 GHz photodetector is used in conjunction with an oscilloscope (Gwinstek: GDS-3352) to investigate the pulse train stability. The generated Q-switched is investigated and analyzed using an MIR spectrometer (Miriad Technologies), an OPM (Thorlabs: PM100D), and a 7.8 GHz radio frequency (RF) spectrum analyzer (Anritsu: MS2683A). The total cavity length is estimated to be ∼13 m.

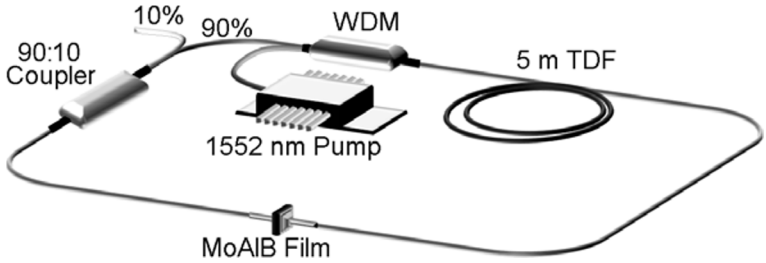

Fig. 3. The schematic configuration of proposed Q-switched TDFL with MoAlB SA.

4. Results and Discussion

At a threshold power of 150 mW, the laser cavity provides the continuous-wave (CW) laser operation. Stable Q-switched laser pulses are successfully produced as the pump power is set between 380 to 436 mW. Even though, some chaotic noise-pulses induced by self-pulsing operation [27] can be observed, the laser cavity is not able to form stable pulsed laser without the integration of SA into the cavity. In Fig. 4 a, we compare the laser wavelength of the TDFL, with and without SA, at a pump power of 436 mW. The central wavelength of the Q-switched spectrum is located at 1974.7 nm, with a 3 dB bandwidth of 9.9 nm. The CW spectrum oscillated at a central wavelength of 1975.7 nm, with a narrower 3 dB bandwidth. The spectral broadening is observed in Q-switched laser due to the self-phase modulation effect inside the TDFL cavity. When the pump power increased beyond 436 mW, the SA becomes saturated and not able to fully recover from the saturation state. As the result, the Q-switched pulses become unstable and dismissed.

In Fig. 4 b, we illustrate the typical pulse train of the designed Q-switched TDFL at a 436 mW pumping power. There are identical pulse trains that indicating the great stability of the Q-switched laser operation. If we further increase the pump power up to 1.5 W and gradually reduced to 436 mW, the dismissed Q-switching is able to recur. Hence, it can be concluded that the SA damage threshold is higher than 1.5 W. The pulse train shows that the Q-switched TDFL has a maximum repetition rate of 57.7 kHz, with a pulse width of 1.79 μs. To investigate the stability of the passively Q-switched operation, we measured the RF spectrum of the Q-switched pulses at a pump power of 436 mW; see Fig. 4 c, where many harmonics with the fundamental frequency at 57.7 kHz are shown. The signal-noise ratio (SNR) of

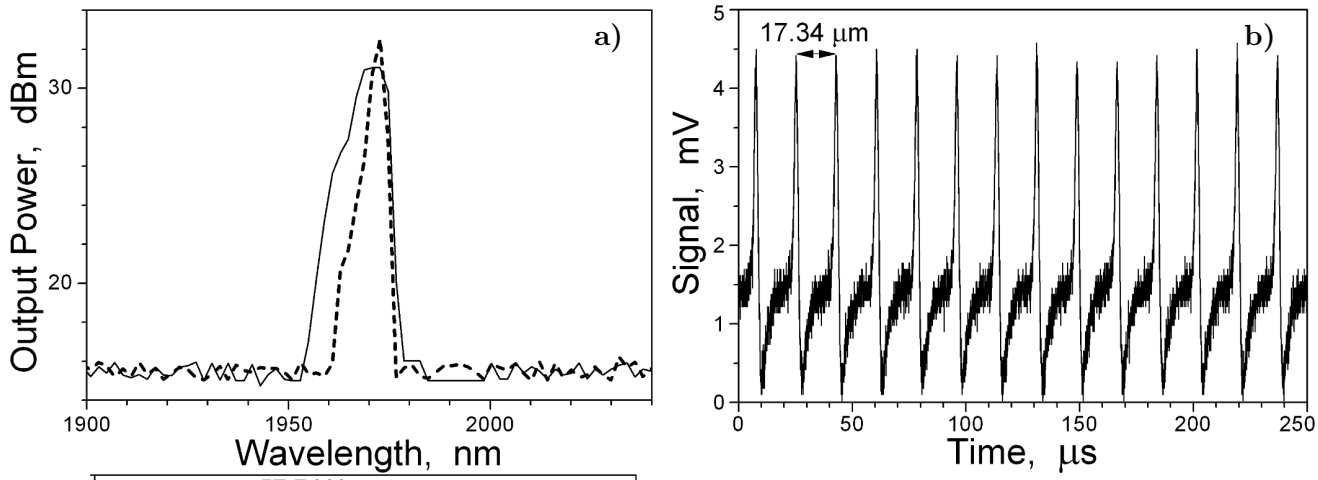

Fig. 4. Characteristics of Q-switched laser pulse operation at a 436 mW pumping at 1552 nm; here, the output spectrum (a) with SA (the solid curve) and without SA (the dashed curve), the pulse train (b), and the RF spectrum (c).

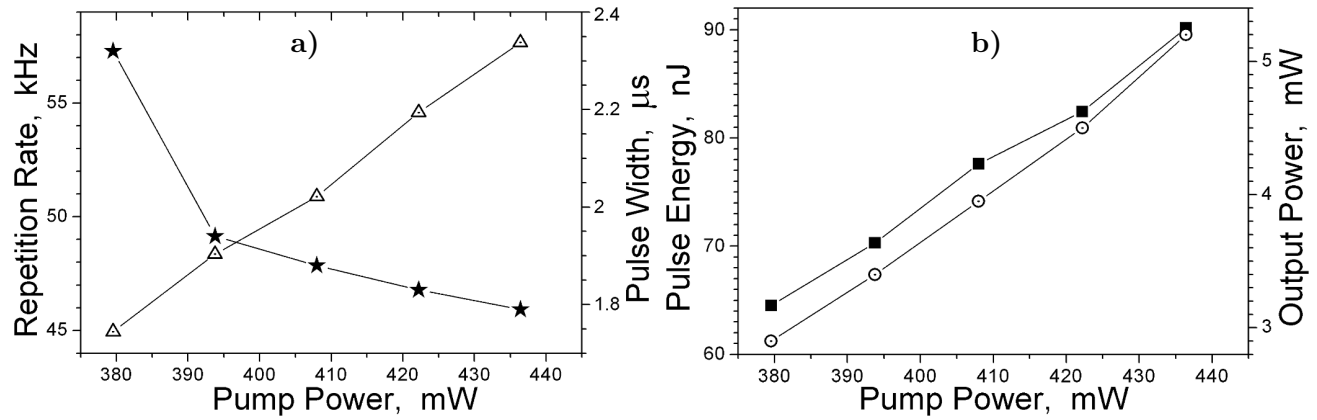

Fig. 5. The proposed Q-switched TDFL performance within a pump power range of 380 to 436 mW; here, (a) the pulse width ($\star$) and repetition rate ($\triangle$) and (b) the pulse energy ($\blacksquare$) and output power ($\odot$).

the fundamental frequency is about 51 dB, that indicates a great stability of the Q-switched operation.

The laser output characteristics of the MoAlB-based Q-switched TDFL are recorded with varying the pump power from 380 to 436 mW; see Fig. 5. One can see in Fig. 5 a that the repetition rate increases from 45.0 to 57.7 kHz, while the pulse width reduces from 2.32 to 1.79 μs with increase in the pump power. Increase in the pump power causes the rising of the photon density growing rate that represents

the storage energy time; this results in forming faster pulses and, thus, we achieve a high repetition rate. In Fig. 5 b, we show the pulse energy and output power of the proposed Q-switched TDFL that are recorded within the pump power range. The pulse energy increases from 64.5 to 90.2 nJ, and the output power raises from 2.9 to 5.2 mW. A linear increase in the output power is proportional to the increase in the TDF gain as the pump power is increased. The larger gain leads to a higher pulse energy due to the quicker build-up progress of the Q-switched pulse.

In Table 1, we compare the performance of the proposed Q-switched TDFL with other 2 μm lasers, which were operated, using other thin-film SAs. The proposed Q-switched TDFL operates at a longer wavelength in the region of 2 μm. On the other hand, the proposed Q-switched TDFL achieves acceptable and comparable values of the repetition rate, pulse duration, and SNR. The proposed Q-switched TDFL has high stable pulses despite the limited pulse energy. In future work, MoAlB-based SA is highly recommended for the formation of mode-locked TDFL, which required further SA and laser cavity optimization.

Table 1. Performance Comparison of Proposed Q-Switched TDFL with Other Reported Works.

SA Material	Wavelength nm	SNR dB	Max. Frequency kHz	Max. Pulse Energy, nJ	Min. Pulse Duration, μs	Max. Output Power, mW	Ref.
Al_2O_3	1950	34.5	40.3	173.5	5.3	–	[28]
GO	1941.7	28	16	18.8	9.8	–	[29]
Antimony	1947	47	23.5	120.1	4.9	2.8	[30]
Alcohol	1885	–	66.7	930	1.5	–	[31]
SWNT	1800	40	67.9	11.9	1.2	–	[32]
MWCNT	1890	–	7.2	–	3.2	–	[33]
Au	1949.19	33.9	21.95	89.8	2.6	1.971	[34]
NiO	1900.52	51	19.58	310	4.24	6	[4]
Our design	1974.7	51	57.7	90.2	1.79	5.2	This work

5. Conclusions

In summary, we proposed and demonstrated a novel Q-switched TDFL using a MoAlB-based SA. The metal–ceramic-based SA was prepared by embedding the MoAlB compound in PVA. The proposed Q-switched TDFL was centered at 1974.7 nm with a maximum repetition rate of 57.7 kHz and a minimum pulse duration of 1.79 μs. The results obtained show that MoAlB SA can be deemed a promising material in photonics technology and TDFL applications. To the best of our knowledge, this is the first report of utilizing MoAlB as a SA for generating pulses in the 2 μm wavelength region.

Acknowledgments

The authors acknowledge the support provided by the Malaysian Ministry of Higher Education under Grant No. FRGS/1/2019/STG02/UM/01/1.

References

1. S. Yao, S. Y. Chen, A. Pal, et al., *Sens. Actuator A Phys.*, **226**, 11 (2015).
2. C. W. Rudy, M. J. F. Digonnet, and R. L. Byer, *Opt. Fiber Technol.*, **20**, 642 (2014).
3. A. A. Shakaty, J. K. Hmood, B. R. Mahdi, et al., *Opt. Laser Technol.*, **146**, 107569 (2022).
4. M. F. M. Rusdi, A. H. A. Rosol, M. F. A. Rahman, et al., *Opt. Commun.*, **447**, 6 (2019).
5. A. A. Al-Azzawi, A. A. Almukhtar, B. A. Hamida, et al., *Results Phys.*, **13**, 102186 (2019).
6. C. G. E. Alfieri, A. Diebold, F. Emaury, et al., *Opt. Express*, **24**, 27587 (2016).
7. A. S. Al-Hiti, A. H. H. Al-Masoodi, S. W. Harun, et al., *Opt. Laser Technol.*, **131**, 106429 (2020).
8. A. S. Al-Hiti, R. Apsari, M. Yasin, and S. W. Harun, *Infrared Phys. Technol.*, **116**, 103788 (2021).
9. X. Peng and Y. Yan, *J. Eur. Opt. Soc. Rapid Publ.*, **17**, 1 (2021).
10. J. Sotor, G. Sobon, K. Grodecki, and K. M. Abramski, *Appl. Phys. Lett.*, **104**, 251112 (2014).
11. Q. Wei, X. Han, H. Zhang, et al., *Appl. Opt.*, **59**, 7792 (2020).
12. Z. Dou, Y. Song, J. Tian, et al., *Opt. Express*, **22**, 24055 (2014).
13. Z. Luo, Y. Huang, J. Weng, et al., *Opt. Express*, **21**, 29516 (2013).
14. J. Sotor, G. Sobon, and K. M. Abramski, *Opt. Express*, **22**, 13244 (2014).
15. A. S. Al-Hiti, A. H. H. Al-Masoodi, W. R. Wong, et al., *Opt. Laser Technol.*, **139**, 106971 (2021).
16. L. Li, Y. Su, Y. Wang, et al., *IEEE J. Sel. Top. Quantum Electron.*, **23**, 44 (2016).
17. P. Wang, D. Hu, K. Zhao, et al., *IEEE J. Sel. Top. Quantum Electron.*, **24**, 1 (2017).
18. M. Liu, W. Liu, and Z. Wei, *J. Lightw. Technol.*, **37**, 3100 (2019).
19. J. Yin, Y. Su, Y. Wang, et al., *Opt. Express*, **25**, 30020 (2017).
20. A. S. Al-Hiti, A. H. H. Al-Masoodi, W. R. Wong, and S. W. Harun, *IET Optoelectron.*, **14**, 278 (2020).
21. K.-X. Huang, B. L. Lu, D. Li, et al., *Appl. Opt.*, **56**, 6427 (2017).
22. A. S. Al-Hiti, M. F. A. Rahman, S. W. Harun, et al., *Opt. Fiber Technol.*, **52**, 101996 (2019).
23. S. P. Munagala, "MAX phases: New class of carbides and nitrides for aerospace structural applications," in: *Aerospace Materials and Material Technologies*, Springer (2017), pp. 455–465.
24. G. Song, "Self-healing of MAX phase ceramics for high temperature applications: Evidence from Ti_3AlC_2," in: *Advances in Science and Technology of* $Mn_1^+AX_n$ *Phases*, Elsevier (2012), pp. 271–288.
25. M. W. Barsoum, *Progress in Solid State Chemistry*, **28**, 201 (2000).
26. A. S. Al-Hiti, M. Yasin, and S. W. Harun, *Opt. Fiber Technol.*, **68**, 102763 (2022).
27. M. Wang, S. Huang, Y.-J. Zeng, et al., *Opt. Mater. Express*, **9**, 4429 (2019).
28. H. Ahmad, A. S. Sharbirin, A. Muhamad, et al., *J. Lightw. Technol.*, **35**, 2470 (2017).
29. H. Ahmad, A. Z. Zulkifli, K. Thambiratnam, and S. W. Harun, *IEEE Photon. J.*, **5**, 1501108 (2013).
30. M. F. A. Rahman, A. A. Latiff, U. Z. M. Zaidi, et al., *Opt. Commun.*, **421**, 99 (2018).
31. B. Ibarra-Escamilla,M. Durán-Sánchez, B. Posada-Ramírez, et al., *IEEE Photon. Technol. Lett.*, **30**, 1768 (2018).
32. H. Ahmad, A. S. Sharbirin, and M. F. Ismail, *Opt. Laser Technol.*, **120**, 105757 (2019).
33. H. Sakata, K. Kimpara, and N. Takahashi, *Electron. Lett.*, **52**, 63 (2016).
34. A. R. Muhammad, R. Zakaria, M. T. Ahmad, et al., *Opt. Fiber Technol.*, **50**, 23 (2019).